

# Magnetic field of an in-plane vortex outside a layered superconductor

J.R. Kirtley

*IBM T.J. Watson Research Center, P.O. Box 218, Yorktown Heights, NY 10598*

V. G. Kogan and J. R. Clem

*Ames Laboratory and Physics Department ISU, Ames, IA 50011*

K.A. Moler

*Dept. of Applied Physics, Stanford University, Stanford, CA 94305*

(May 4, 2018)

## Abstract

We present the solution to London's equations for the magnetic fields of a vortex oriented parallel to the planes, and normal to a crystal face, of a layered superconductor. These expressions account for flux spreading at the superconducting surface, which can change the apparent size of the vortex along the planes by as much as 30%. We compare these expressions with experimental results.

## A. Introduction

Recently, scanning SQUID microscope magnetic imaging of interlayer vortices trapped between the planes of layered superconductors has been used to make direct measurements of the interlayer penetration depth in several layered superconductors [1], [2], [3], [4]. These experiments provide local measurements of the interlayer supercurrent density, which have

implications for the validity of the interlayer tunneling model [5] as a candidate mechanism for superconductivity in the high critical temperature cuprate superconductors.

To date the quantitative modelling of these experiments has assumed that the vortex fields at the superconductor-vacuum interface are the same as those in the bulk, neglecting the well known effect that the magnetic fields from vortices spread as they approach the superconductor-vacuum surface from within the superconductor. Exact theoretical expressions exist for a vortex in an isotropic London's model [6]. For a vortex oriented perpendicular to the surface in a superconductor with an isotropic penetration depth  $\lambda$ , the fields above the surface can be approximated by a magnetic monopole located a distance  $\lambda$  below the surface [6], [7]. This means that the spatial extent of the magnetic fields at the surface is larger than in the bulk of the superconductor. If the bulk expressions were used to fit data at the surface, the fitted value of the penetration depth would be longer than the real value. This effect must be accounted for in making quantitative estimates of the penetration depths by magnetic imaging measurements. For this purpose it is useful to examine vortex spreading at the surface for a highly anisotropic superconductor, since recent experiments have studied vortices in superconductors with  $\lambda_c/\lambda_{ab} \sim 10-100$ .

It is well known that the anisotropic London model is appropriate for describing a stack of Josephson-coupled superconducting layers at length scales large compared to the interlayer spacing. In this paper we present an exact solution of London's equations for a straight vortex approaching a superconductor-vacuum interface normal to the interface, in an anisotropic superconductor. We show how flux spreading near this interface effects the magnetic fields above the interface, and show that there is good agreement between these theoretical results and scanning SQUID microscope measurements on single crystals of the layered high- $T_c$  cuprate superconductor  $Tl_2Ba_2CuO_{6+\delta}$  (Tl-2201) [1].

## B. The model

A method for finding the field distribution of a straight vortex crossing a plane surface of an anisotropic superconductor has been developed in Ref. [8]. We will outline this method and apply it to the case of a vortex, oriented along  $b$  in the  $ab$  plane of a uniaxial material, which crosses the plane face  $ca$  of the crystal. For a vortex not too close to the crystal corners, the crystal surface  $ca$  can be taken as an infinite plane. We choose the coordinates  $x, y, z$  corresponding to  $c, a, b$  of the crystal as shown in Fig. 1. Then the mass tensor is diagonal:  $m_{xx} = m_3, m_{yy} = m_{zz} = m_1$ . The standard normalization  $m_1^2 m_3 = 1$  is implied. The method consists of solving London's equations for the field inside the superconductor and matching the result to a solution of Maxwell's equations in the vacuum outside the sample. For the isotropic case, the problem is simplified by the cylindrical symmetry of the field distribution [6,9]. This is not the case for anisotropic materials, and a more general approach is needed.

Inside the superconductor, the field  $\mathbf{h}(\mathbf{r}, z)$ , with  $\mathbf{r} = \{x, y\}$ , satisfies the London equations [10]:

$$h_i - \frac{4\pi}{c} \lambda^2 m_{k\ell} e_{i\ell s} \frac{\partial j_k}{\partial x_s} = \phi_0 \delta(\mathbf{r}) \delta_{iz}. \quad (1)$$

Here,  $\mathbf{j}$  is the current density,  $\phi_0 = hc/2e$  is the superconducting flux quantum, and the average penetration depth  $\lambda = (\lambda_{ab}^2 \lambda_c)^{1/3}$  ( $\lambda_{ab}^2 = m_1 \lambda^2$ ,  $\lambda_c^2 = m_3 \lambda^2$ ).

Deep inside the superconductor, the field  $\mathbf{h}(\mathbf{r})$  has only a  $z$  component. However, near the exit from the sample at  $z = 0$ , the vortex “opens up” and  $h_x, h_y$  are no longer zero. In other words, Eq. (1) is a system of three linear differential equations for  $h_x, h_y$ , and  $h_z$  with a non-zero right-hand side (RHS). The general solution is then

$$\mathbf{h} = \mathbf{h}^{(0)} + \mathbf{h}^{(v)}, \quad (2)$$

where  $\mathbf{h}^{(0)}$  solves the homogeneous system with zero RHS, whereas  $\mathbf{h}^{(v)}$  is a particular solution of the full system (1). The latter can be taken as the field of an infinitely long

unperturbed vortex along  $z$ ; this assures correct singular behavior at the vortex axis. The Fourier transform of this field is

$$\mathbf{h}^{(v)} = \frac{\phi_0}{1 + \lambda_{ab}^2 k_x^2 + \lambda_c^2 k_y^2} \hat{\mathbf{z}}. \quad (3)$$

With this choice of  $\mathbf{h}^{(v)}$ , the field  $\mathbf{h}^{(0)}$  is the correction due to the surface of the unperturbed vortex field  $\mathbf{h}^{(v)}$ . We note that the Clem-Coffey result for a vortex parallel to the layers of a Josephson coupled layered superconductor reduces to  $\mathbf{h}^{(v)}$  if one disregards the core correction [11].

Because the only sample boundary is parallel to the plane  $xy$ , we Fourier transform Eq. (1) with respect to  $x, y$ . We are then left with the system of equations for  $\mathbf{h}(\mathbf{k}, z) = \int d\mathbf{r} \exp(-i\mathbf{k} \cdot \mathbf{r}) \mathbf{h}(\mathbf{r}, z)$ :

$$\begin{aligned} m_1 h_x'' - (1 + m_1 k_y^2) h_x + m_1 k_x k_y h_y - i m_1 k_x h_z' &= 0, \\ m_1 k_x k_y h_x + m_3 h_y'' - (1 + m_1 k_x^2) h_y - i m_3 k_y h_z' &= 0, \\ i m_1 k_x h_x' + i m_3 k_y h_y' + (1 + m_1 k_x^2 + m_3 k_y^2) h_z &= \phi_0. \end{aligned} \quad (4)$$

For brevity, we have set the average  $\lambda$  as the unit of length so that  $\lambda_{ab}^2 = \lambda^2 m_1$  and  $\lambda_c^2 = \lambda^2 m_3$  are replaced with  $m_1$  and  $m_3$ ; the prime in the above equations denotes  $d/dz$ . The field  $\mathbf{h}^{(0)}(\mathbf{k}, z)$  satisfies the *homogeneous* system of *linear second order ordinary differential* (with respect to the variable  $z$ ) equations, i.e., it is a linear combination of exponential functions of  $z$ :

$$\mathbf{h}^{(0)}(\mathbf{k}, z) = \sum_n \mathbf{H}^{(n)}(\mathbf{k}) e^{\alpha_n z}. \quad (5)$$

The  $z$  independent coefficients  $\mathbf{H}^{(n)}(\mathbf{k})$  and  $\alpha_n(\mathbf{k})$  are still to be determined. Each term in the sum (5) should satisfy separately the system (4) with zero RHS. Omitting the label  $n$  we write this system as

$$\Delta_{ij} H_j = 0 \quad (6)$$

with a symmetric matrix  $\Delta_{ij}$ :

$$\begin{aligned}
\Delta_{xx} &= 1 + m_1 k_y^2 - m_1 \alpha^2, \\
\Delta_{xy} &= -m_1 k_x k_y, \\
\Delta_{xz} &= i m_1 k_x \alpha, \\
\Delta_{yy} &= 1 + m_1 k_x^2 - m_3 \alpha^2, \\
\Delta_{yz} &= i m_3 k_y \alpha, \\
\Delta_{zz} &= 1 + m_1 k_x^2 + m_3 k_y^2.
\end{aligned} \tag{7}$$

The determinant of this matrix must be zero, which provides all possible values of  $\alpha$ :

$$\alpha_{1,2} = \pm \left( \frac{1 + m_1 k^2}{m_1} \right)^{1/2}, \tag{8}$$

$$\alpha_{3,4} = \pm \left( \frac{1 + m_1 k_x^2 + m_3 k_y^2}{m_3} \right)^{1/2}. \tag{9}$$

Deep inside the superconductor, the surface correction  $\mathbf{h}^{(0)}(z \rightarrow -\infty)$  must vanish, implying  $\alpha_1$  and  $\alpha_3$  must be positive. The homogeneous system (6) allows one to express (for each of these  $\alpha$ 's) two out of three components  $H_i$  in terms of the third. We obtain after simple algebra:

$$H_x^{(1)} = i \frac{1 + m_1 k_x^2}{m_1 k_x \alpha_1} H_z^{(1)}, \quad H_y^{(1)} = i \frac{k_y}{\alpha_1} H_z^{(1)}; \tag{10}$$

$$H_x^{(3)} = 0, \quad H_y^{(3)} = i \frac{\alpha_3}{k_y} H_z^{(3)}. \tag{11}$$

Thus, the field inside the sample will be determined completely after  $H_z^{(1)}$  and  $H_z^{(3)}$  are found from the boundary conditions at the sample surface.

The field outside the sample is described by  $\text{div}\mathbf{h} = 0$  and  $\text{curl}\mathbf{h} = 0$ , so that one looks for  $\mathbf{h} = \nabla\varphi$  with  $\nabla^2\varphi = 0$ . The general solution of Laplace's equation which vanishes at  $z \rightarrow \infty$  is

$$\varphi(\mathbf{r}, z) = \int \frac{d^2\mathbf{k}}{(2\pi)^2} \varphi(\mathbf{k}) e^{i\mathbf{k}\cdot\mathbf{r} - kz}. \tag{12}$$

The 2D Fourier transform is defined by

$$\varphi(\mathbf{k}) = e^{kz} \int d^2\mathbf{r} \varphi(\mathbf{r}, z) e^{-i\mathbf{k}\cdot\mathbf{r}}. \tag{13}$$

The boundary conditions at the free surface  $z = 0$  consist of continuity of the three field components:

$$\begin{aligned} ik_x \varphi &= H_x^{(1)} + H_x^{(3)}, \\ ik_y \varphi &= H_y^{(1)} + H_y^{(3)}, \\ -k \varphi &= h_z^{(v)} + H_z^{(1)} + H_z^{(3)}. \end{aligned} \quad (14)$$

The components  $H_{x,y}^{(1,3)}$  are expressed in terms of  $H_z^{(1,3)}$  in Eqs. (10), (11), so that the system (14) can be solved to find  $\varphi$  along with all  $H_i$ 's. We are interested here primarily in the field outside the sample:

$$\varphi(\mathbf{k}) = -\frac{\phi_0 (1 + m_1 k_x^2)}{m_3 \alpha_3 [m_1 k_x^2 \alpha_3 (k + \alpha_1) + k \alpha_3 + k_y^2]}. \quad (15)$$

It is readily verified that for the isotropic material Eq. (15) reduces to the known result by Pearl:  $\varphi = -\phi_0 / \alpha_{is} k (k + \alpha_{is})$  where  $\alpha_{is}$  is the isotropic version of either  $\alpha_1$  or  $\alpha_3$  [6].

Since *outside* the sample  $\mathbf{h} = \nabla \varphi$ , we have

$$h_{x,y}(\mathbf{k}) = ik_{x,y} \varphi(\mathbf{k}), \quad h_z(\mathbf{k}) = -k \varphi(\mathbf{k}). \quad (16)$$

Then, for example, the

$$h_z(\mathbf{r}, z) = -\int \frac{d^2 \mathbf{k}}{(2\pi)^2} k \varphi(\mathbf{k}) e^{i\mathbf{k} \cdot \mathbf{r} - kz}. \quad (17)$$

In particular, the total magnetic flux through any plane  $z = z_0$  is given by  $h_z(k = 0, z_0) = \phi_0$  as expected.

The field *inside* the sample is given by Eqs. (2), (3), (5). The coefficients  $\mathbf{H}^{(1,3)}$  in

$$\mathbf{h}^{(0)}(\mathbf{k}, z) = \mathbf{H}^{(1)} e^{\alpha_1 z} + \mathbf{H}^{(3)} e^{\alpha_3 z} \quad (18)$$

are obtained by solving (14), (10), and (11):

$$\mathbf{H}^{(1)} = \varphi(\mathbf{k}) \left\{ ik_x, i \frac{m_1 k_x^2 k_y}{1 + m_1 k_x^2}, \frac{m_1 k_x^2 \alpha_1}{1 + m_1 k_x^2} \right\}, \quad (19)$$

$$\mathbf{H}^{(3)} = \varphi(\mathbf{k}) \left\{ 0, \frac{ik_y}{1 + m_1 k_x^2}, \frac{k_y^2}{\alpha_3 (1 + m_1 k_x^2)} \right\}. \quad (20)$$

Thus, for example,

$$h_x(\mathbf{r}, z) = \int \frac{d^2\mathbf{k}}{(2\pi)^2} ik_x \varphi(\mathbf{k}) e^{i\mathbf{k}\cdot\mathbf{r} + \alpha_1 z}. \quad (21)$$

For what follows, we will only concern ourselves with the fields outside of the superconductor. In the experiment of Ref. [1], the component  $h_z$  was probed with a SQUID pickup loop which was much larger than the penetration depth  $\lambda_{ab}$ . One therefore expects the instrument to measure a flux nearly equal to the pickup loop size times

$$\mathcal{H}_z(x, y) = \int_{-\infty}^{\infty} h_z(x, y, z) dx. \quad (22)$$

The vortex spreads as it approaches from below the superconducting surface in the  $x$ -direction as well as in the  $y$ -direction; nevertheless numerical estimates show that under typical conditions the experimental signal is well represented by Eq. (22). Then we obtain:

$$\frac{\mathcal{H}_z(y, z)}{\phi_0} = \int_{-\infty}^{\infty} \frac{dk_y}{2\pi} \frac{e^{ik_y y - |k_y|z}}{m_3 \alpha (\alpha + |k_y|)} \quad (23)$$

with  $\alpha = \alpha_3(k_x = 0) = (m_3^{-1} + k_y^2)^{1/2}$ . In conventional units,

$$\frac{\mathcal{H}_z(y, z)}{\phi_0} = \int_{-\infty}^{\infty} \frac{dk_y}{2\pi} \frac{e^{ik_y y - |k_y|z}}{\alpha (\alpha + \lambda_c |k_y|)} \quad (24)$$

with  $\alpha = (1 + \lambda_c^2 k_y^2)^{1/2}$ . It is worth noting that the quantity  $\mathcal{H}_z(y, z)$  depends only on  $\lambda_c$ .

After the substitution  $\lambda_c k_y = \sinh u$ , Eq. (24) takes the form

$$\begin{aligned} \pi \lambda_c \frac{\mathcal{H}_z(x, y)}{\phi_0} &= \int_0^{\infty} du e^{-u - z' \sinh u} \cos(y' \sinh u) \\ &= \operatorname{Re} \int_0^{\infty} du e^{-u - w \sinh u} \\ &= \operatorname{Re} \left[ \frac{1}{w} + \frac{\pi}{2} (\mathbf{E}_1(w) + Y_1(w)) \right], \end{aligned} \quad (25)$$

Here,  $y' = y/\lambda_c$ ,  $z' = z/\lambda_c$ , and  $w = (z + iy)/\lambda_c$ ;  $\mathbf{E}_1$  and  $Y_1$  are Weber's and Neumann functions, see Ref. [12].

For  $|w| \ll 1$  (both  $y$  and  $z$  are small relative to  $\lambda_c$ ) we have [12]:

$$\begin{aligned} \pi \lambda_c \frac{\mathcal{H}_z(y, z)}{\phi_0} &= \operatorname{Re} \left[ 1 + \frac{w}{2} \left( \ln \frac{w}{2} + \gamma - \frac{1}{2} \right) \right] \\ &= 1 + \frac{z}{2\lambda_c} \left( \ln \frac{\sqrt{y^2 + z^2}}{2\lambda_c} + 0.077 \right) - \frac{y}{2\lambda_c} \tan^{-1} \frac{y}{z} \end{aligned} \quad (26)$$

( $\gamma = 0.577$  is Euler's constant). If  $|w| \gg 1$  (at least one of  $y$  or  $z$  is large relative to  $\lambda_c$ ), we obtain:

$$\begin{aligned}\pi\lambda_c \frac{\mathcal{H}_z(y, z)}{\phi_0} &= \operatorname{Re} \left[ \frac{1}{w} - \frac{1}{w^2} + O(|w|^{-4}) \right] \\ &= \frac{z\lambda_c}{y^2 + z^2} - \frac{(z^2 - y^2)\lambda_c^2}{(z^2 + y^2)^2} + \dots\end{aligned}\quad (27)$$

At large distances from the vortex exit, the second term can be neglected and  $\lambda_c$  drops out of the result; this is expected since the field there is approaching the Coulomb form with no trace of material properties.

To form a complete picture of the field distribution outside the sample, we imagine that the same SQUID probe is oriented in the  $xz$  plane so that the  $y$ -component of the field (integrated over the probe area) is measured. Then the SQUID flux will be nearly equal to the pickup loop size times

$$\begin{aligned}\mathcal{H}_y(y, z) &= \int_{-\infty}^{\infty} h_y(x, y, z) dx \\ &= \int_{-\infty}^{\infty} \frac{dk_y}{2\pi} ik_y \varphi(0, k_y) e^{ik_y y - k_y z}.\end{aligned}\quad (28)$$

The two-dimensional field  $\vec{\mathcal{H}}$  satisfies  $\operatorname{div} \vec{\mathcal{H}} = \operatorname{curl} \vec{\mathcal{H}} = 0$ . Hence, it can be written as  $\vec{\mathcal{H}} = \nabla \Phi$  with  $\nabla^2 \Phi = 0$ . This implies that  $\mathcal{H}_z$  and  $\mathcal{H}_y$  are real and imaginary parts of the same analytic function given in Eq. (25): [13]

$$\mathcal{H}_y(y, z) = \frac{\phi_0}{\pi\lambda_c} \operatorname{Im} \left\{ \frac{1}{w} + \frac{\pi}{2} [\mathbf{E}_1(w) + Y_1(w)] \right\}.\quad (29)$$

In particular, the asymptotic form of this function for  $w \gg 1$  can be written as

$$\frac{1}{w} - \frac{1}{w^2} \approx \frac{1}{w+1},\quad (30)$$

which implies that at large distances the field  $\vec{\mathcal{H}}$  behaves as a field of a 2D "charge" situated at  $z = -\lambda_c$ .

### C. Results

Figure 2(a) shows streamlines of  $\vec{\mathcal{H}}(y, z)$  for a single anisotropic vortex centered at  $x = 0$ ,  $y = 0$ . These streamlines were generated numerically as follows: the starting points of the

lines were at  $z/\lambda_c = -3$ , with a spacing in  $y$  between the lines proportional to  $(\partial \mathcal{H}_z / \partial y)^{-1}$  at  $z/\lambda_c = -3$ . Small steps  $z = z + \Delta z$ ,  $y = y + \Delta y$ , with  $\Delta z = \delta \sin \theta$ ,  $\Delta y = \delta \cos \theta$ , were generated, with  $\theta = \tan^{-1}(\mathcal{H}_z(y, z) / \mathcal{H}_y(y, z))$ . The fields were recalculated at the new positions, and then the process was repeated until  $|z/\lambda_c| > 3$  or  $|y/\lambda_c| > 3$ . Figure 2(b) shows the results if field spreading below the surface is neglected:

$$b_z(x, y, z < 0) = \frac{\phi_0}{2\pi\lambda_{ab}\lambda_c} K_0(\tilde{R}), \quad (31)$$

where  $K_0$  is a modified Bessel function of the second kind of order 0,  $\tilde{R} = [(s/2\lambda_{ab})^2 + (x/\lambda_{ab})^2 + (y/\lambda_c)^2]^{1/2}$ , and  $s$  is the interplanar spacing [11]. For  $s \ll \lambda_{ab}$ , Eq. (31) has the Fourier transform given in Eq. (3). The fields for  $z > 0$  are given by

$$b_z(\mathbf{r}, z) = \int \frac{d^2\mathbf{k}}{(2\pi)^2} b_z(\mathbf{k}) e^{i\mathbf{k}\cdot\mathbf{r}-kz}, \quad (32)$$

where

$$b_z(\mathbf{k}) = \int d^2\mathbf{k} b_z(x, y, z = 0) e^{-i\mathbf{k}\cdot\mathbf{r}}. \quad (33)$$

[14]. The fields in the  $x$  and  $y$  directions are treated similarly, using the relations  $b_x(\mathbf{k}) = -ik_x b_z(\mathbf{k})/k$ , and  $b_y(\mathbf{k}) = -ik_y b_z(\mathbf{k})/k$ . The calculated fields were integrated over  $x$  and streamlines were generated just as for the exact London expressions. This is the procedure used to model the experimental results in Ref. [1]. In both cases the fields extend into the vacuum nearly isotropically at large distances, as if a point monopole source were placed near  $z = -\lambda_c$ . In the full treatment, Figure 2(a), the fields spread as the vortex approaches the surface from inside the superconductor.

A one-dimensional rendering of our results above the surface of the superconductor is shown in Figure 3, which plots  $\pi\lambda_c \mathcal{H}_z(y, z) / \phi_0$  as a function of  $y/\lambda_c$  for several values of  $z/\lambda_c$ . For comparison, the results neglecting vortex spreading are also shown. Note that  $\mathcal{H}_z(0, 0)$ , which approximately indicates the peak signal in an experiment, is overestimated by a factor of  $\pi/2$  if vortex spreading is neglected. Also, the full width at half-maximum of the flux contour is  $1.87\lambda_c$  for the full theory, while it is  $1.37\lambda_c$  if flux spreading is neglected. Therefore the neglect of flux spreading could result in an overestimate of  $\lambda_c$  by 30%.

#### D. Comparison with experiment

Previous analyses of experimental data [1], [2], neglected the effect of vortex spreading at the surface. In retrospect, this neglect was not unreasonable, given the quantitative agreement between the interlayer coupling strength obtained from vortex imaging measurements and from the Josephson plasma resonance [2]. With the full theory presented in this paper, it is now possible to quantitatively examine this assumption. However, we note that there are additional systematic experimental uncertainties in this technique. These errors include the effect of macroscopic screening currents which may create a slightly inhomogeneous background, a relative angle of 10-20 degrees between the surface of the superconductor and the SQUID pickup loop, the uncertainty in the exact value of the height of the pickup loop, and some effect of the leads to the pickup loop on the effective shape of the pickup loop. We estimate that these errors may also be as large as 30%.

Figure 4 shows grey-scale images of 5 interlayer vortices in Tl-2201 magnetically imaged using a scanning SQUID microscope [1]. In these experiments the experimental signal is equal to the integrated magnetic flux through the pickup loop. The vortices appear elliptical in shape, with the long axis (parallel to the planes) nearly vertical in these images. The spatial extent of the vortex images perpendicular to the planes is limited simply by the size of the pickup loop. The spatial extent parallel to the planes is set primarily by the interplanar penetration depth. Figure 5 shows cross-sections through the experimental data along the direction parallel to the planes as indicated by the dashed lines in Figure 4.

To generate a theoretical expression for fitting the experiment results, we use the full expression (Eq. (15)) for the magnetic fields, taking the a-axis penetration depth equal to  $0.17\mu\text{m}$  [15]. An evaluation of Eq. (15) gives the  $z$ -component of the field at a given height  $z_0$  above the sample surface. This field is then numerically integrated over the shape of the pickup loop to obtain the total theoretical flux  $\Phi_s(x, y, z)$  through the pickup loop as a function of the pickup loop position and the c-axis penetration depth  $\lambda_c$ . In this case the pickup loop used was a square  $8.2\mu\text{m}$  on a side, with a  $1\mu\text{m}$  linewidth, and a superconducting

shield  $5\mu\text{m}$  wide which extends to the top corner of the pickup loop, as indicated by the inset of Figure 4. For our modelling we add to the flux through the pickup loop one third of the flux intercepting an area  $5\mu\text{m}$  by  $5\mu\text{m}$  on a side, starting at the upper corner of the pickup loop, to account for flux focussing effects from the superconducting shield. The solid lines in Figure 5 are best fits of the cross section  $\Phi_s(x = 0, y, z = z_0)$  to the experimental data, using the interlayer penetration  $\lambda_c$ , the height of the pickup loop  $z_0$ , and an offset flux, representing a small uncertainty of the background signal, as free parameters. The best fit values for each vortex are displayed in the figure, with uncertainties assigned using a doubling of the  $\chi^2$  value as a criterion. Reasonable agreement is obtained between experimental and theoretical cross-sections. The average value for  $\lambda_c$ , using a weighting inversely proportional to the square of the uncertainties, is  $\lambda_c = 18.3 \pm 3\mu\text{m}$ .

For comparison, a similar analysis of the same vortices neglecting the effect of vortex spreading resulted in a weighted average best-fit value of  $\lambda_c = 19 \pm 2\mu\text{m}$ . This comparison is surprising at first, since the theoretical FWHM at the surface is reduced by 30% when the vortex spreading is neglected. However, the uncertain value of the height of the pickup loop compensates for the assumption of negligible vortex spreading below the surface. When the spreading below the surface is neglected, the fitting routine compensates by picking a higher value of  $z_0$ , thereby moving the spreading to the vacuum rather than the superconductor.

In conclusion, we have presented a solution to London's equation for the case of an interlayer vortex approaching a superconducting surface normal to the surface and parallel to the planes. This model is appropriate for experiments which magnetically image interlayer vortices. Good agreement with available experiments is obtained with this model, allowing the quantitative determination of the interlayer penetration depths from these measurements.

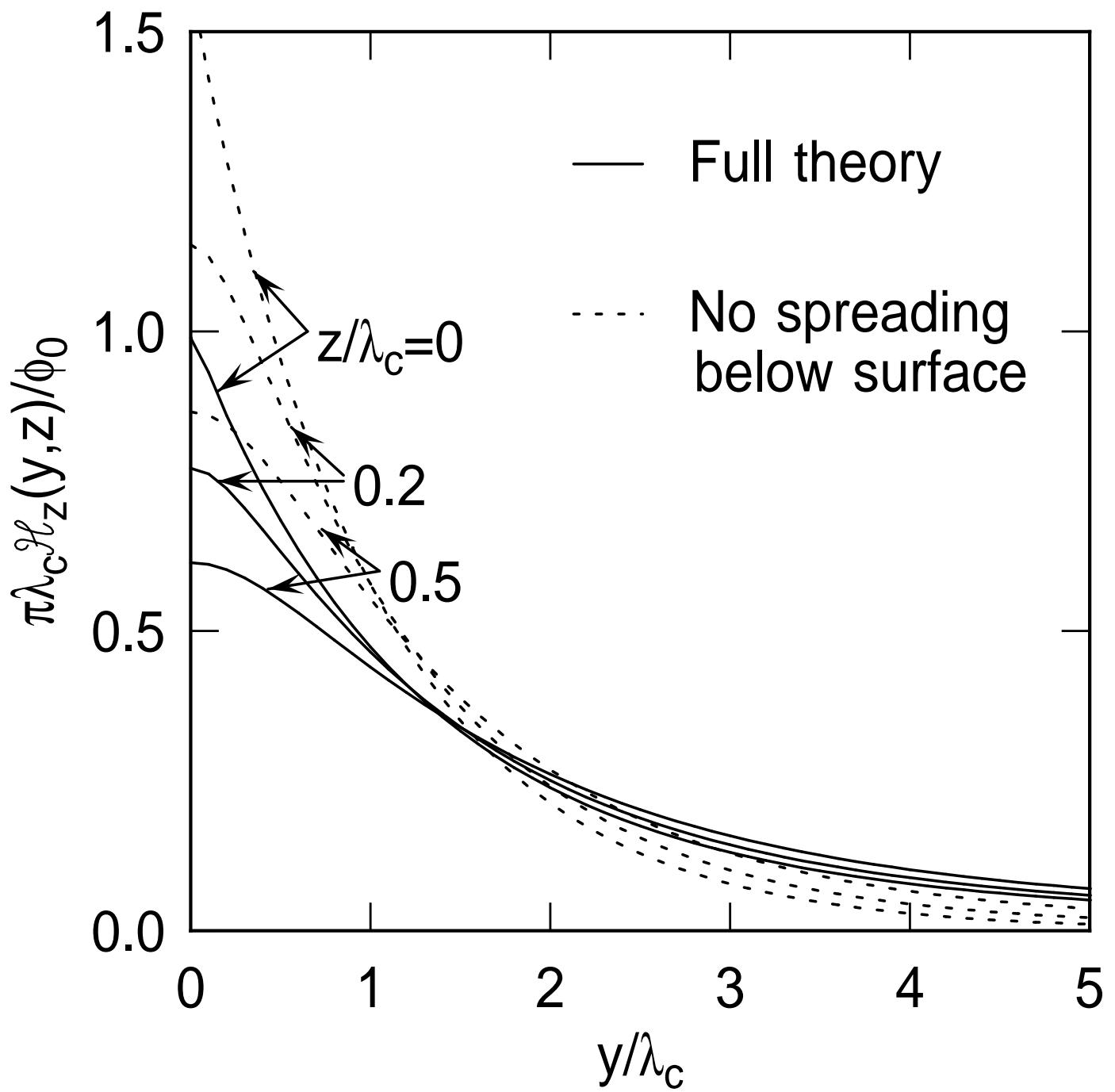
We would like to thank D.G. Hinks, T.W. Li, and Ming Xu for supplying the Tl-2201 crystals used for the SQUID images shown in this paper. We would also like to thank M.B. Ketchen for the design, and M. Bhushan for the fabrication, of the SQUIDs used here.

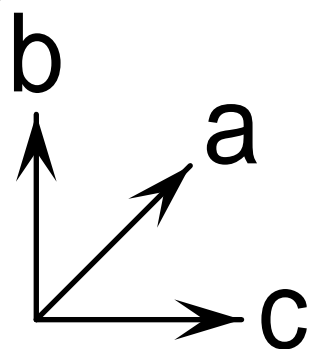
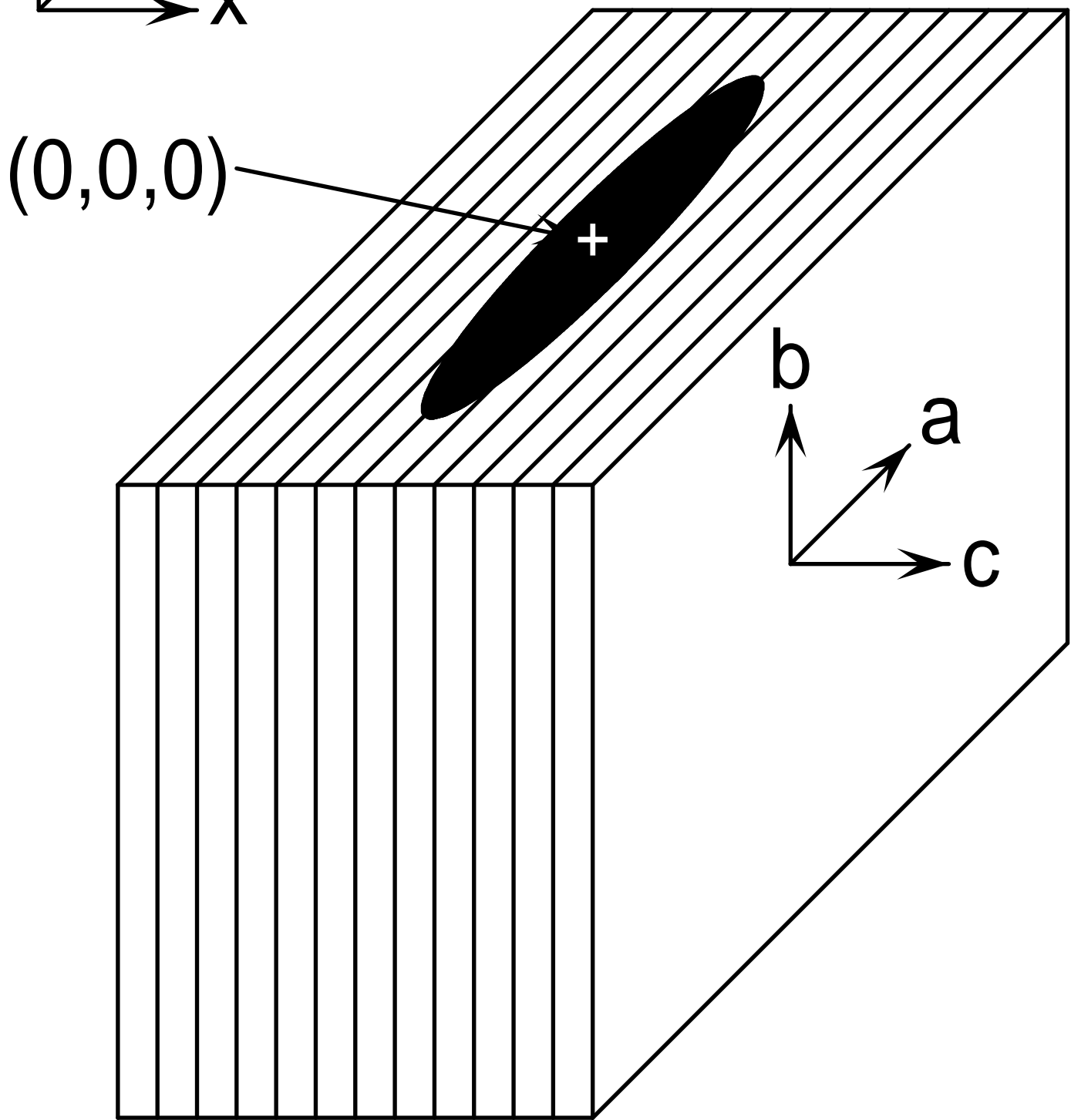
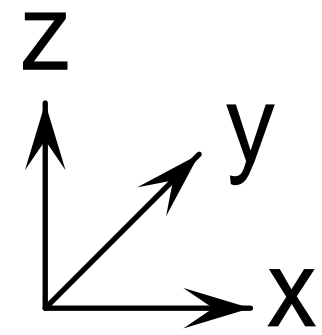
## REFERENCES

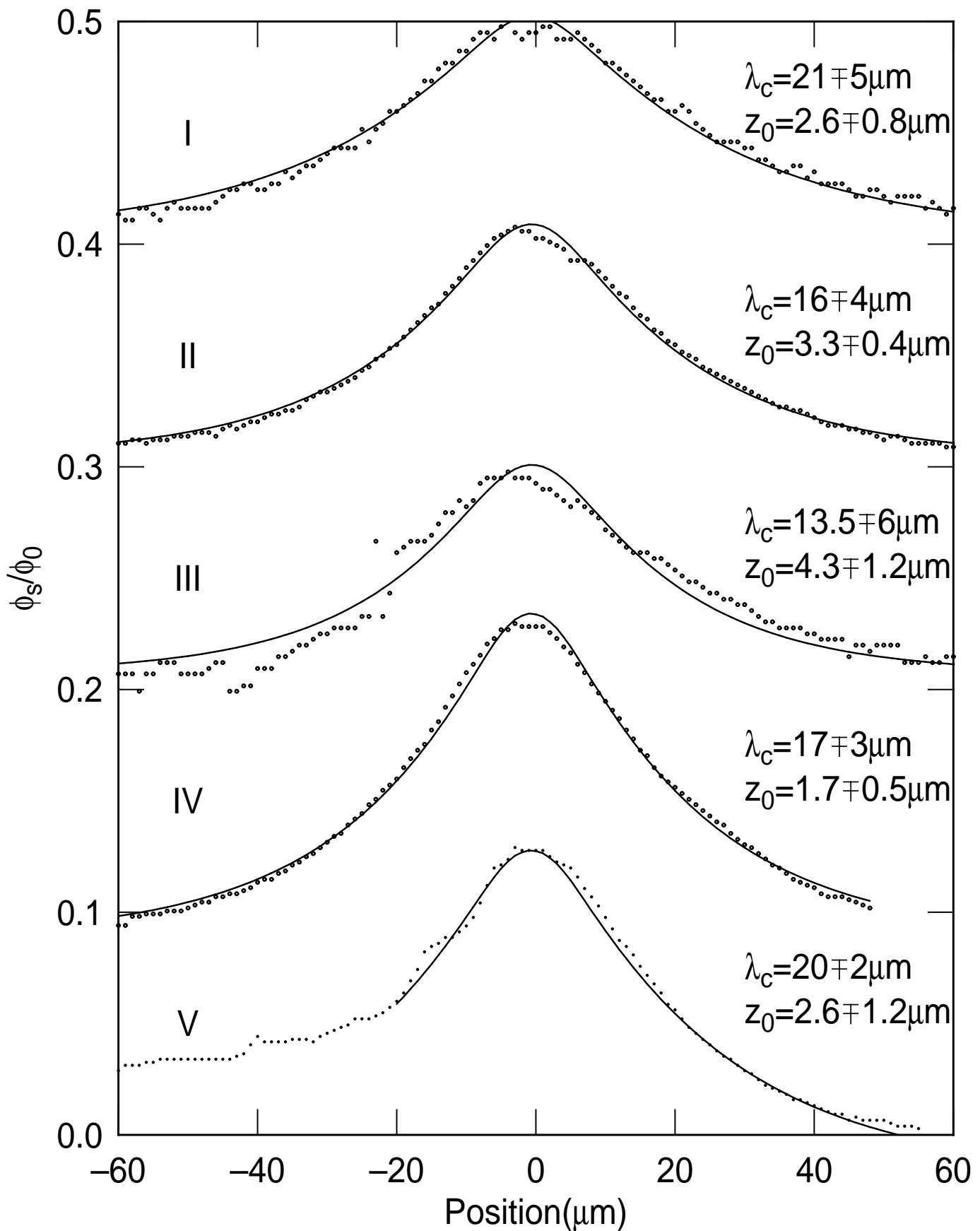
- [1] K. A. Moler, J. R. Kirtley, D. G. Hinks, T. W. Li, and Ming Xu, *Science* **279**, 1193 (1998).
- [2] A.A. Tsvetkov *et al.* *Nature* in press.
- [3] J.R. Kirtley, K.A. Moler, G. Villard and A. Maignan, *Phys. Rev. Lett.* in press.
- [4] J.R. Kirtley, K.A. Moler, J.M. Williams and J.A. Schlueter, preprint.
- [5] J. Wheatley, T. Hsu, and P.W. Anderson, *Nature* **333**, 121 (1988); P.W. Anderson, *Physica C* **185**, 11 (1991); *Phys. Rev. Lett.* **67**, 660 (1991); *Science* **256**, 1526 (1992); S. Chakravarty, A. Sudbø, P.W. Anderson, and S. Strong, *ibid* **261**, 331 (1993).
- [6] J. Pearl, *J. Appl. Phys.* **37**, 4139 (1966).
- [7] A.M. Chang *et al.* *Europhys. Lett.* **20**, 645 (1992).
- [8] V. G. Kogan, A. Yu. Simonov, and M. Ledvij, *Phys. Rev. B* **48**, 392 (1993).
- [9] J. R. Clem, *Phys. Rev. B* **1**, 2140 (1970).
- [10] V. G. Kogan, *Phys. Rev. B* **24**, 1572 (1981).
- [11] J. R. Clem and M. Coffey, *Phys. Rev. B* **42**, 6209 (1990).
- [12] I. S. Gradshteyn and I. M. Ryzhik, *Tables of Integrals, Series and Products*, Academic Press, NY 1965.
- [13] L. D. Landau and E. M. Lifshitz, *Electrodynamics of Continuous Media*, Pergamon, NY 1984
- [14] Bradley J. Roth, Nestor G. Sepulveda, and John P. Wikswo, *J. Appl. Phys.* **65**, 361 (1988).
- [15] F. Zuo *et al.* *Phys. Rev. B* **47**, 8327 (1993).

## Figure Captions

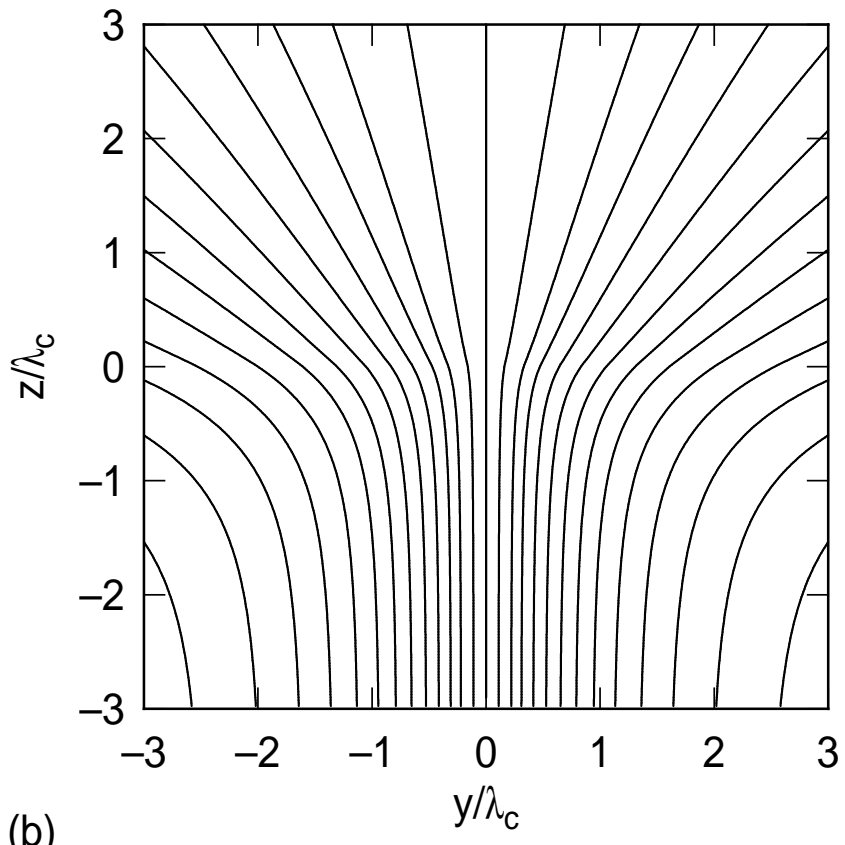
1. Geometry and axes used in this paper. A single vortex, centered at  $x = 0, y = 0$ , emerges normally to the  $ac$  face of the crystal located at  $z = 0$ .
2. Stream-line mapping of  $\vec{\mathcal{H}}(y, z)$ , the magnetic field integrated over  $x$ , for a single interlayer vortex shown in Fig. 1. The spacing of the stream lines is proportional to  $(\partial\mathcal{H}_z/\partial y)^{-1}$  at  $z = -3\lambda_c$ . Fig. 2a is the present model, which includes vortex spreading; Fig. 2b is for a model which neglects field spreading below the surface.
3. Plot of  $\mathcal{H}_z(y, z)$  for a single interlayer vortex normal to the superconducting surface  $z = 0$ , as a function of  $y/\lambda_c$ , for fixed  $z$  values, where  $y$  is the distance from the center of the vortex along a plane direction, and  $\lambda_c$  is the interlayer penetration depth.
4. Grey-scale images of 5 interlayer vortices in the high- $T_c$  cuprate superconductor Tl-2201. The scaling corresponds to  $0.11\phi_0$ (I),  $0.16\phi_0$ (II),  $0.13\phi_0$ (III),  $0.22\phi_0$ (IV), and  $0.19\phi_0$ (V) full-scale variation from black to white in the integrated flux through the pickup loop.
5. Cross-sections along the plane directions through the images of Figure 4. Each successive curve is offset by 0.1 unit for clarity. The dots are the data; the lines are fits to the present model as described in the text.







(a)



(b)

